ABSORBANCE AND FLUORESCENCE STUDIES ON PORPHYRIN NANOSTRUCTURES (PNR) AS LIGHT HARVESTERS IN DYE SENSITIZED SOLAR CELLS

George, R. C.,[a,b] Egharevba, G. O.,[a] and Nyokong, T.[b]

[a]Department of Chemistry, Obafemi Awolowo University, Ile-Ife, Nigeria
[b]Department of Chemistry, Rhodes University, Grahamstown, South Africa
[*]Corresponding Author: reama.george@gmail.com
(Received: 12th Sept., 2013; Accepted: 23rd Sept., 2013)

ABSTRACT

Porphyrin nanorods (PNR) were fabricated by electrostatic self-assembly of two oppositely charge molecules and the compounds used were free base meso-tetra-(4-sulphonatephenyl) porphyrin ($H_2TPPS_4^{4-}$) and metallo meso-tetra (4-N-methylpyridyl) porphyrin ($MTMPyP^{4+}$) (M = Sn, Mn, Co, In). The aim of this work was to study some photophysical properties of PNR for application as light harvester in dye sensitized solar cells. These properties included absorbance, fluorescence, and fluorescence quantum yield and lifetime. The results of Transmission Electron Microscope (TEM) images showed the formation of nanorods. Electronic Spectra of the PNR revealed J-aggregation bands at 492 nm and accompanied by a band at 712 nm. All the porphyrin nanostructures produced fluorescence at 670 nm when excited at 430 nm and each spectrum had a hidden band at 730 nm. The fluorescence quantum yields were low but deconvolution of the bi-exponential decay curves showed the existence of two species with lifetimes of ~3 ns and ~200 ps.

Keywords: Porphyrin, Nanorods, Fluorescence, Fluorescence Quantum Yield, Lifetimes, J-aggregates

INTRODUCTION

The first Dye Sensitized Solar Cell (DSSC) was made in 1972 with chlorophyll sensitized zinc oxide electrodes (Tributsch and Calvin, 1971). Ruthenium and Osmium polypyridyl complexes as light harvesters have higher efficiencies compared to other organic dyes. Nevertheless these metals are rare and quite toxic (Gratzel, 2004). Porphyrins are among the many alternative organic complexes being investigated for the role of light harvesting in DSSC. The advantages porphyrins have are their similarity to chlorophyll, structural tenability (Chou *et al*., 2000; Kral *et al.,* 2006; Tachibana *et al.* 2000; Wamser *et al.,* 2002) as well as thermal stability which makes them suitable for rooftops applications. The photosynthetic structure of plants are 3-D whereas those of solar cells are designed to be single-layered making the process 2-D. Attempts have been made to use multichromophoric systems are still not successful (Burrell *et al.,* 2001). However porphyrin dimers which are covalently linked together have an increase of 20 % light harvesting efficiency using a thinner photoanode of 2.5 μM compared to those of multichromophoric systems (Mozer *et al.,* 2009).

In this work porphyin nanorods (PNR) were fabricated with the porphyrin molecules lying side-to-side in an orderly manner of J-aggregation (Ribo *et al.,* 1994). Studies have shown that J-aggregate dyes allow for electron transportation, producing highly delocalized exciton and therefore act as light harvesters via excitation energy transfer (EET) (Atkins, 1996). Therefore the potential applications of PNRs as light harvesters for solar cells were investigated by studying their absorbance and fluorescence properties as well as fluorescence life time of their excited state.

EXPERIMENTAL

Free base meso tetra-(4-phenyl) porphyrin (H_2TPP) was first synthesized according to an earlier method described by Nascimento *et al.* (2007) and then sulphonated to free base meso-tetra-(4-sulphonatephenyl) porphyrin ($H_2TPPS_4^{4-}$), Fig. 1a, according to the process described by Srivastava and Tsutsui (1973). The sulphonation of H_2TPP made the compound negatively charged and water soluble. The first stage of the synthesis of metallo meso-tetra-(4-N-methylpyridyl) porphyrin (MTMePyP, M = Sn, In, Co, Mn), Fig.

1b, was the synthesis of meso-tetra-(4-pyridyl) porphyrin (TPyP) (Nascimento *et al.,* 2007). This was followed by the metallation of TPyP to metallo meso-tetra-(4-pyridyl) porphyrin (MTPyP) using $SnCl_2$, $Mn(CH_3COO)_2$, $CoCl_2$, and $InCl_3$ were carried out according to the procedures described elsewhere (Alder *et al.,* 1970; Herman *et al.,* 1978; Hong *et al.,* 1996). Finally, the four metalloporphyrins were quaternized using the same procedure as described for the quaternized 2,(3)-tetra(oxopyridine) phthalocyaninato chloroindium(III) (QInPyPc) (Durmus and Nyokong, 2007). Quaternization is the addition of a methyl group on the pyridine N-atom, making them positively charged and therefore soluble in water.

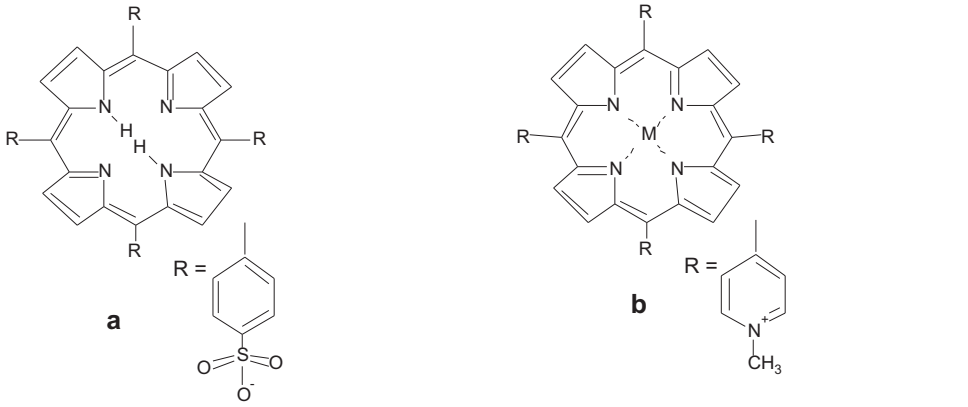

ms-tetraphenylsulfonate porphyrin

ms-tetra(N-methyl-4-pyridyl) porphyrin

M = Sn, Mn, Co, In

Fig.1 Structures of the Negatively and Positively Charged Porphyrin Molecules.

Porphyrin nanorods were fabricated by electrostatic self-assembly of two oppositely charged porphyrin molecules. $H_2TTPS_4^{4-}$ (10.5 x 10^{-6} M) was first prepared in an acidic solution (HCl 0.02 M) so as to protonate the central cavity, creating a dipositive centre.

$$H_2TPPS_4^{4-} + 2H^+ \rightleftharpoons H_4TPPS_4^{2-}$$

$H_4TTPS_4^{2-}$ (10.5 x 10^{-6} M, 6 ml) was mixed with solution of each of the positively charged molecules $SnTMPyP^{4+}$, $CoTMPyP^{4+}$, $MnTMPyP^{4+}$, $InTMPyP^{4+}$ (3.5 x 10^{-6} M, 6 ml) and left in the dark for 3 days (Wang *et al.,* 2004). At the end of the third day a green coloured colloidal suspension of the aggregates were obtained and labelled as: $H_4TTPS_4^{2-}$-$SnTMPyP^{4+}$ (HT-Sn); $H_4TTPS_4^{2-}$-$CoTMPyP^{4+}$ (HT-Co); $H_4TTPS_4^{2-}$-$MnTMPyP^{4+}$ (HT-Mn); $H_4TTPS_4^{2-}$-$InTMPyP^{4+}$ (HT-In). TEM imaging of these nanostructures was obtained with JEOL 1210 (80KV). The colloidal suspension of PNR 10 µl were deposited onto carbon coated grids and air dried before imaging. UV-Vis electronic spectra of PNR were recorded using Shimadzu UV-2550 spectrophotometer (path length 10 mm, quartz cell).

Fluorescence spectra of the porphyrin nanostructures were obtained using Varian Eclipse Spectrofluorimeter (path length 10 mm, quartz cell) and by applying an excitation wavelength of 430 nm. Fluorescence quantum (Φ_F) yields values were determined by comparative method using the equation below and fluorescein as standard (Magde *et al.,* 2002).

$$\phi_F = \phi_{F(Std)} \frac{F \cdot A_{(Std)} \cdot \eta^2}{F_{Std} \cdot A \cdot \eta^2_{(Std)}} \qquad (1)$$

where F and F_{Std} are the areas under the fluorescence curves of the PNR and fluorescein respectively. A and A_{Std} are the absorbances of the sample and standard at the excitation wavelength, and η and η_{Std} are the refractive indices of the solvents (water) used for the sample and standard, respectively (Aldofas *et al.,* 2008). The standard has fluorescence quantum yield, F = 0.925 in 0.1M NaOH (Magde *et al.,* 2002). Furthermore absorbance intensities were kept below 1.0 for

both the standard and the PNR to allow excitation of the aggregate as against the usual mono molecular excitation of absorbance intensity less than 0.05.

Fluorescence lifetimes τ_f of the PNR were measured using a Time-Correlated Single-Photon Counting setup (TCSPC) (Fluo Time 200, Picoquant GMbH) with a diode laser as excitation source (LDH-P-670) driven by PDL 800-B, 670 nm, 20MHz repetition rate, Picoquant GmbHv and excitation intensities were kept constant at 2.0 $x10^{16}$ photon-cm^{-2} per pulse.

RESULTS AND DISCUSSION

The TEM images, Fig. 2, show that the porphyrin molecules self assembled into rod-like structure in the nanoscale not nanotubes as reported by Wang *et al.*, (2004). This has been attributed to the use of 4-N-methylpyridyl porphyrin instead of hydrogen-bonding protonated pyridine groups (Medforth *et al.,* 2009). Although there were no observable correlations amongst the TEM images of the PNR in relation to the central metals being transition metals or not, the observed differences as seen could be due to the different properties of each metal as well as the possible effects of ligands on the geometry of the metals and symmetry of the ring.

The UV-Vis spectra of the porphyrin nanorods showed that they absorbed from 400 nm to 800 nm having very broad bands. The B-band occurred around 434 nm and the J-aggregate band at 492 nm accompanied by a band at 712 nm, (Fig. 3). These peaks of the porphyrin nanorods are red shifted compared to those of the homo-aggregates $H_4TPPS_4^{2-}$ and this result is in agreement with other studies (Wang *et al.*, 2004; George *et al.,* 2010). The broadness of these bands is due to an increase in number of vibronic state generated through aggregation (Koti *et al.,* 2003). J-aggregates of $H_4TPPS_4^{2-}$ are created by the electrostatic interaction between negatively charged sulphonate group of one molecule and positively charged centre of another (Ribo *et al.,* 1994). It has been presumed that the mechanism for growth of PNR aggregates begins with 1-d J-aggregation of $H_4TPPS_4^{2-}$ followed by electrostatic interactions between this 1-d layer and the positively charged molecules creating the 3-d porphyrin nanorods (George *et al.,* 2010; Billo 2001).

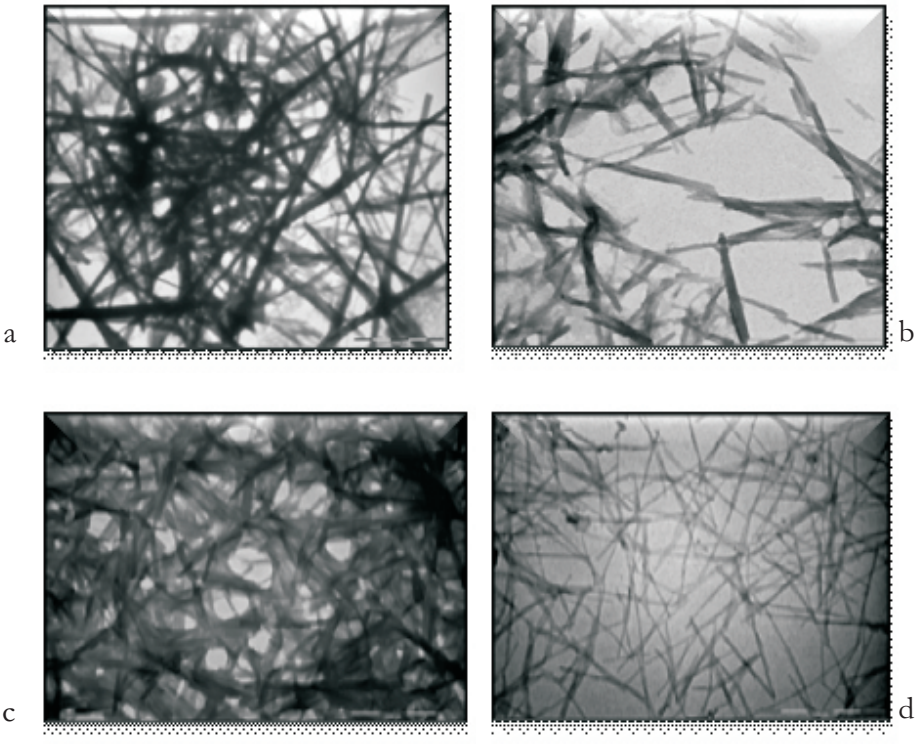

Fig. 2 TEM Images of PNR (a) $H_4TPPS_4^{2-}$ $SnTMPyP^{4+}$ (HT-Sn) (b) $H_4TPPS_4^{2-}$ $InTMPyP^{4+}$ (HT-In) (c) $H_4TPPS_4^{2-}$ $MnTMPyP^{4+}$ (HT-Mn) (d) $H_4TPPS_4^{2-}$ $CoTMPyP^{4+}$ (HT-Co).

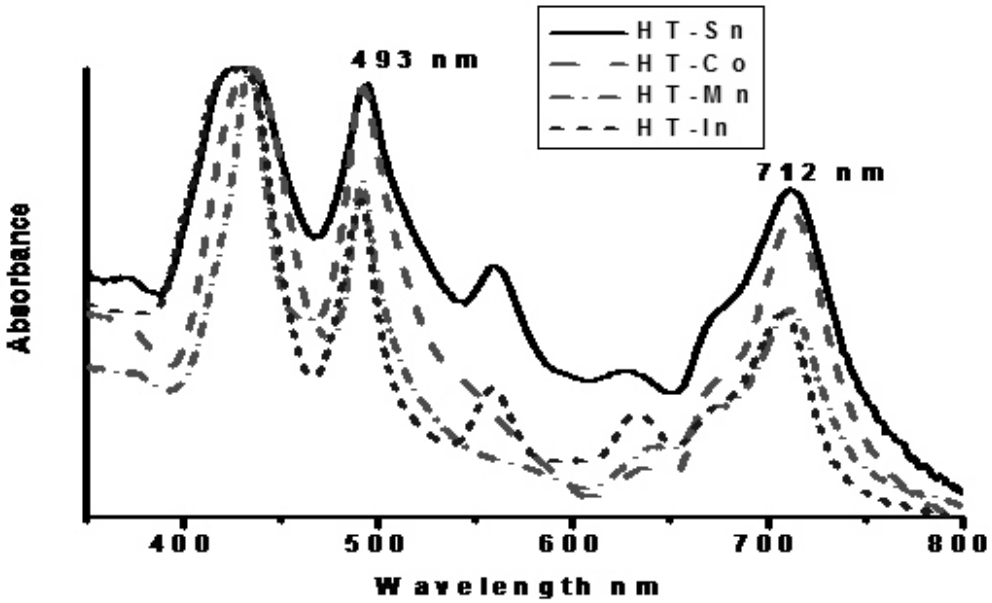

Fig. 3 Electronic Spectra of PNR.

According to molecular exciton model (Kasha *et al.,* 1965), van der Waals interactions between the oppositely charged molecules result in splitting of the exciton state from E to E' and E''. The transition dipoles of J-aggregates are in-line therefore the in-phase dipole interactions are attractive producing E' (allowed) lowering the energy level while the out-of-phase dipole interactions are repulsive raising the energy level of the exciton state E'' (forbidden). Hence electronic spectra of J-aggregates are red shift compared to the monomer (Kasha *et al.,* 1965). The red shift of the J-aggregate bands of PNR showed that the allowed exciton states of the PNR are lower in energy than those of the homo-aggregates of $H_4TPPS_4^{2-}$. The advantage that porphyrin molecules have is their high absorption coefficient and although it decreases with aggregation, these nanorods have wide absorption in the visible region which would increase their efficiency as a light harvester (Gratzel, 2004).

Excitation of the colloidal suspension of PNR at 430 nm produced a single broad fluorescence peak at 670 nm and a shoulder around 730 nm, which made them asymmetrical indicative of one or more hidden bands (Billo, 2001) (Fig 4). The spectra obtained were of the same shape as those obtained by Gupta *et al.* (2011), who worked with $H_4TPPS_4^{2-}$-FeTMPyP. The difference between the fluorescence spectra of the J-aggregate of $H_4TPPS_4^{2-}$ and the PNR is the hidden shoulder present in the fluorescence spectra of the PNR as well as the decrease in fluorescence intensity which is due to quenching of fluorescence as a caused by aggregation (Lakowicz, 2002).

Previous studies have shown that the fluorescence band at 670 nm was produced by $H_4TPPS_4^{2-}$ molecules not within PNR network. While the hidden band at 730 nm was produced by the PNR (Atkins, 1996; Gouterman, 1978). Excitation of the colloidal suspension of PNR with energy lose the wavelength of the absorption maximum of the J-aggregates band (488 nm) produced very weak fluorescence at 730 nm.

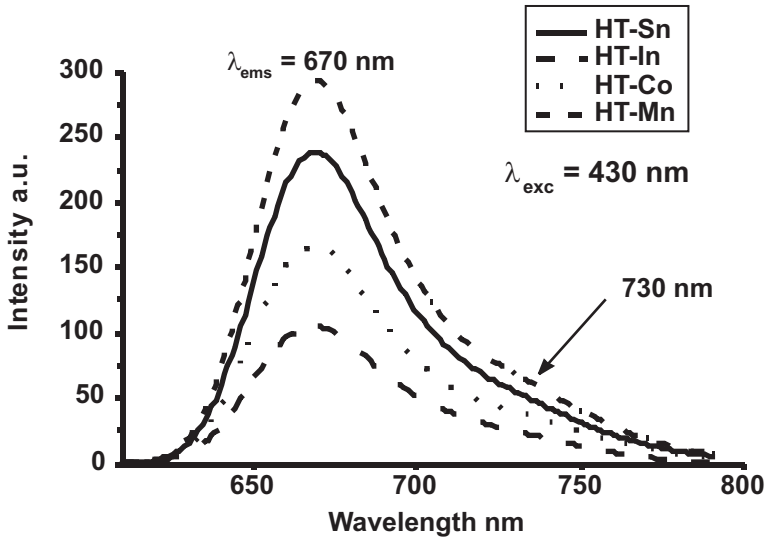

Fig. 4 Fluorescence Spectra of PNR

Fluorescence quantum yield, Φ_F shows the population of excited molecules undergoing fluorescence and fluorescence lifetimes show the lifetime of the excited state before deactivation. The fluorescence lifetimes together with the fluorescence quantum yields are listed in Table 1. For the porphyin nanorods (PNR), bi-exponential decay was applied for the fitting of the fluorescence kinetics measured, Fig. 5, and decay times were obtained after deconvolution of the fluorescence decay curve with the instrument response functions.

The two lifetimes around ~ 3 ns and ~ 200 ps observed indicates the presence of two fluorescencing species in the sample and similar results were reported for the study of J-aggregate of H_4TPPS_4 (Gratzel, 2004; Kelbuakas *et al.,* 2001). The efficiency of PNR in the excited state to inject the electrons into the conduction band of the semiconductor is in competition with the natural relaxation process to the ground state of the molecules. Studies have shown that about 60 % of the electrons are injected from the singlet state have lifetimes in femtoseconds and the rest from the triplet state occurring at slower pace (Gratzel, 2004). The two set of excitons produced from the PNR are in the singlet state occurring within the required time frame[2] having above 70 % of the photon with a lifetime of over 200 ps. This suggests that much of the excited molecules stay in the first excited state and thus could transfer the electron to the semiconductor as required in DSSC.

Table 1 Summary of Fluorescence Quantum Yield and the Half Lives of Each PNR

PNR	Φ_F	τ_1 (ns)	A_1 (Cnts)	τ_2 (ps)	A_2 (Cnts)	Total (Cnts)
HT-Sn	0.02	3.27 ± 0.01	1699 (0.15)	220	9266 (0.85)	10965
HT-In	0.01	3.29± 0.05	1748 (0.14)	200	11137 (0.86)	12885
HT-Mn	0.02	3.39± 0.02	4401 (0.29)	214	10532 (0.71)	14933
HT-Co	0.01	3.37± 0.01	4936 (0.33)	259	9877 (0.67)	13813

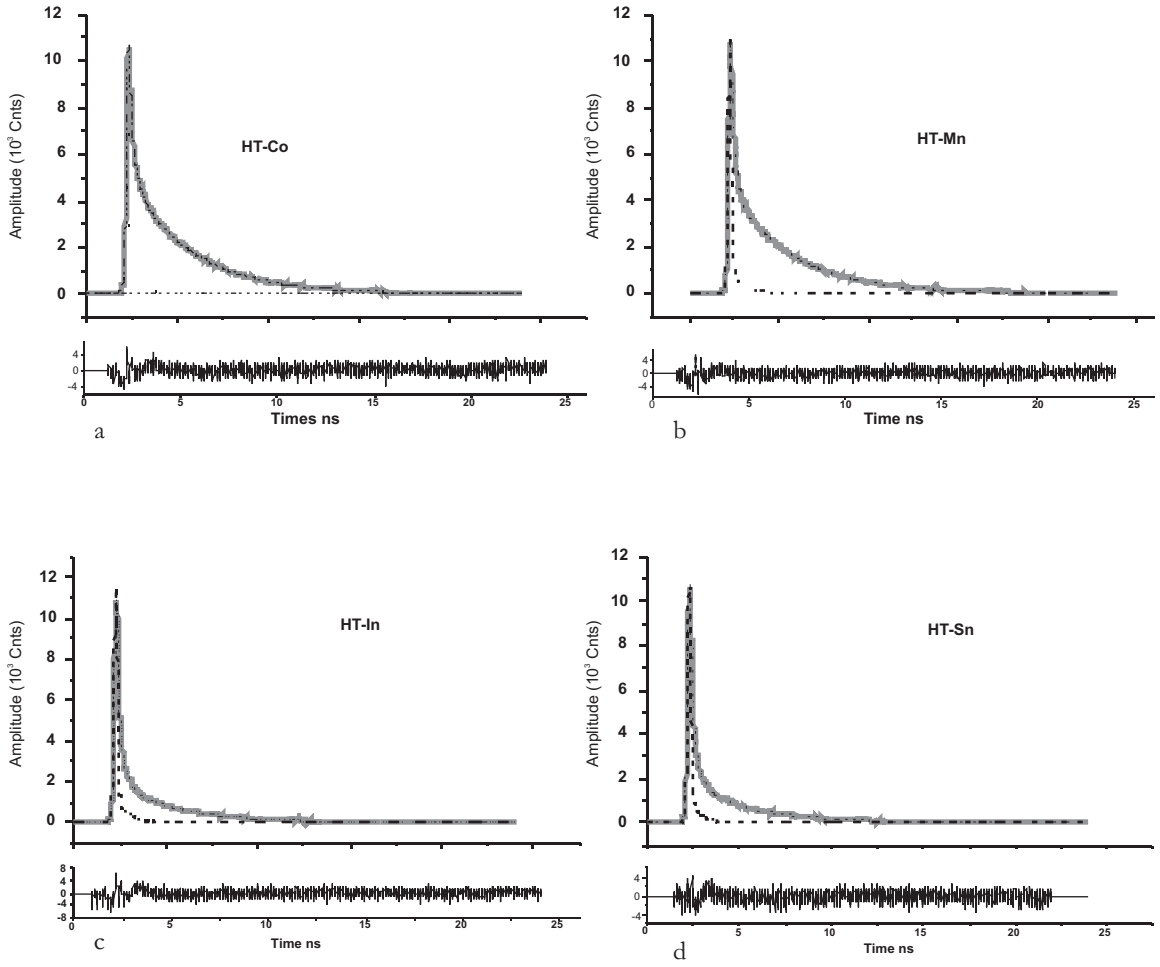

Fig.5 Fluorescence Excitation Kinetics of PNR. A Fit to the Bi-Exponential Law with Time. The Dash Line Represents the Instrument Response Function. (FWHM ˜ 300 ns). (a. HT-Co, b. HT-Mn, c. HT-In, d. HT-Sn).

The low quantum yield is as a result of very low concentration of diprotonated monomers of tetrasulphonate porphyrin ($H_4TPPS_4^{2-}$) present in the colloid suspension (Kelbuakas et al., 2001). Another factor responsible for the low quantum yield is aggregation (in PNR) which creates low lying energy states therefore radiationless decays occur more rapidily than the radiative decay (Lakowicz, 2002; Gouterman, 1978; Kelbuakas et al., 2001). This might be of an advantage in DSSC because of the presence of a large number of molecular orbitals at low lying energy states. Thus there is a higher probability of finding excitons at energy levels favourable for injection into the conduction band of the semi-conductor (Gratzel, 2004).

The lifetime of ~3 ns is attributed to the excited state of the monomer diprotonated $H_2TPPS_4^{4-}$ in the collodial suspension (Kelbuakas et al., 2001). However under the experimental condition used in this work by applying an excitation intensity higher than of 10^{14} photon/cm^2 per pulse (i.e. 2.0 x10^{16} photon/cm^2 per pulse), such high intensities have been reported to produce singlet-singlet annihilation that occur within the aggregate domain as the excitons hop within the porphyrin aggregate network (Kelbuakas et al., 2001).

$$S_1 + S_1 \rightarrow S_1 + \text{heat}$$

The short-lived component (~200 ps) was also attributed to the natural exciton lifetime within the aggregate in the absence of annihilation as the time was too short for excitons to interact with each other (Kelbuakas et al., 2001). It was proposed that the short-lived exciton might be charge migrating because the excited states in J-

aggregates are Frenkel exciton delocalized over a given number of dye molecules. Such intermolecular resonance interactions responsible for the exciton delocalization favours energy migration within the PNR network could make them work efficiently as light harvesters (Hongzehen et al., 2009). However the lower population of electrons (photon count) of the long-lived species could deplete further due to the annihilation process before injection as more of the short-live species proceed into the conduction band.

CONCLUSION

Porphyrin nanorods have shown good response as light harvesters for DSSC. They have a wide absorption range i.e. the entire visible region. Although the fluorescence quantum yield was low, the life time of the two excited states are slow enough to allow ejection of an electron from the excited state into the conduction band of the semi-conductor. The intense overlap of the molecular orbital during aggregation results in band formation which should provide energy state high enough above the conduction band of semi conductor to allow this transfer. It is presumed the exciton produced within the porphyrin nanorods although short-lived have a higher probability of being injected into the conduction band of the semi-conductor used in the DSSC.

ACKNOWLEDGEMENT

This work was supported by the Department of Science and Technology (DST) and National Research Foundation (NRF), South Africa through DST/NRF South African Research Chairs Initiative for Professor of Medicinal Chemistry and Nanotechnology and Rhodes University. Reama George thanks Organization for Women in Science for the Developing World (OWSD) for a bursary.

REFERENCES

Alder, A. D., Longo, F. R., Kampas, F. and Kim J. 1970. On The Preparation of Metalloporphyrins. *J. Inorg. Nucl. Chem.* 32, 2443-2447.

Adolfas, K., Wang, G. and Wang, L. 2008. Measurements of the Flourescence Quantum Yeld Using a Spectrometer with an Intergrating Sphere Detector. *J. Res. Natl. Inst. Stand. Techno.* 113, 17-28.

Atkins, D. L. 1996. Cyanines And Porphyrins. In: J-Aggregates Structure and Exciton Emission Dynamics of Molecular Aggregates. Kobayashi, T. [ed.]. *Singapore : World Scientific,* 67-94.

Billo, J. E. 2001. Deconvolution of spectra. In: *Excel for chemistry: A Comprehensive Guide 2.* New York : Wiley-VCH, 19, 318-322.

Burrell, A. K., Officer, D. L., Plieger, P. G. and Reid, D. C. W. 2001. Synthetic Routes to Multiporphyrin Arrays. *Chem. Rev.* 101, 2751-2796.

Chou, J-H., Kosal, M. E., Nalwa, H. S., Rakow, N.A. And Suslick, K.S. 2000. Application of Porphyrins and Metalloporphyrins to Material Chemistry. In: *The Porphyrin Handbook* Smith, K., Guilard, R. And Kadish, K. [Eds.]., New York : Academic Press, 6, 43-131.

Durmus, M. and Nyokong, T. 2007. Synthesis, Photophysical and Photochemical Studies of New Water Soluble Indium (III) Phthalochyanines. *Photochem. Photobiol. Sci.* 665-670.

George, R. C., Egharevba, G. O., and Nyokong, T. 2010. Spectroscopic Studies of Nanostructures of Negatively Charged Free Base Porphyrin and Positively Charged Tin Porphyrin. *Polyhedron* 29, 1469-1474.

Gouterman, M. 1978. Optical Spectra and Electronic Structure of Porphyrin and Related Rings. *The Porphyrins.* D. Dolphin [ed.]. New York : Academic 3, 1-11

Gratzel, M. 2004. Dye-Sensitized Solar Cells. *J. Photochem. Photobio. C: Photochem Rev.* 4, 145-153.

Gutpa, J., Lim, X., Sow, C.-H. and Vijayan, C. 2011. Micropattering of Porphyrin Nanotubes ThinFilms Using Focused Laser Writing. *J. Nanosci. Nanotechnol.* 11, 4029-4033.

Herrman, O., Medhi, S.H., and Corsini A. 1978. Heterogeneous Metal-Insertion: A Novel Reaction with Porphyrins. *Can. J. Chem.* 56, 1084-1087.

Hong, T.-N., Sheu, Y.-H., Jang, K.-W., Chen, J.-H., Wang, S.-S., Wang, J.-.C and Wang S. L. 1996. A New Synthesis of Acetoato Porphyrinato Indium(III) from In (III) Oxide and X-ray Crystal Structure of

In(tpyp)(OAc) and In (tmpyp)(OAc). *Polyhedron* 15, 2647-2652.

Hongzehen, L., Camacho, R., Tian, Y., Kaiser, T. E., Wurthner, F. and Scheblykin, I. G. 2009. Collective Fluorescence Blinking in Linear J-Aggregates Assisted by Long-Distance Exciton Migration. *Nano Lett.* 1-7.

Kasha, M., Rawls, H. R. and EL-Bayomi, M. A. 1965. The Exciton Model in Molecular Spectroscopy. *Pure Appl. Chem.* 11, 371-392.

Kelbauskas, L., Bagdanos, S., Dietel W. and Rotomskis, R. 2003. Excitation Relaxation and Structure of $TPPS_4$ J-Aggregates. *J. Lumin.* 101, 253-262.

Kim, D. Holten, D. and Gouterman, M. 1984. Evidence from Picosecond Transient Absorption and Kinetic Studies of Charge-Transfer States in Copper(II) Porphyrins. *J. Am Chem Soc.* 106, 2793-2798.

Koti, A. S. R., Taneja, J. and Periasamy, N. 2003. Control of Coherence Length and Aggregate Size in J-aggregate of Porphyrins. *Chem. Phys. Lett.* 375, 171-178.

Kral, V. Kralova, R. Kaplaner, R. Briza, T. and Martaskek, P. 2006. Quo Vadis Porphyrin Chemistry. *Physiol. Res.* 55, 3-26.

Lakowicz, J. R. 1999. Introduction to Fluorescence. In: *Principles of Fluorescene Spectroscopy*. New York : Kluwer Academic/Plenum Publisher, pp 1-20.

Magde, D. Wong, R. and Seybold, G. 2002. Fluorescence Quantum Yeild and their Relation to Lifetime of Rhodamine 6G and Flourescein in Nine Solvents: Improving Absolute Standards for Quantum Yields. *Photochem. Photobio.* 75, 327-338.

Medforth, C. J., Wang, Z., Martin, K. E., Song, Y., Jacobsen, J. L. and Shelnutt, J. A. 2009. Self-Assembled Porphyrin Nanostructures. *Chem. Comm.* 47, 7241-7428.

Mozer, A. J., Griffith, M. J., Tsekouras, G., Wagner, P., Wallace, G. G. and Mori, S. 2009. Zn-Zn Porphyrin Dimer-Sensitized Solar Cells: Toward 3-D Light Harvesting. *J. Am. Chem. Soc.* 131, 15621-15623.

Rio, Y., Rodriguez-Morade, M. S. and Torres, T. 2008. Modulating the Electronic Properties of Porphyrinoids: A Voyage from the Violet to the Infrared Regions of the Electromagnetic Spectrum. *Org. Biomol. Chem.* 1877-1894.

Tachibana, Y., Haque, S. A., Mercer, I. P., Durrant, J. R. and Klug, D. R. 2000. Electron Injection and Recombination in Dye Sensitized Nanocrystalline Titanium Dioxide Films: A Comparison of Ruthenium Bipyridyl and Porphyrin Sensitizer Dyes. *J. Phys. Chem.* 104, 1198-1205

Tributsch, H. and Calvin, M. 1971. Electrochemistry of Excited Molecules: Photo-Electrochemical Reactions of Chlorophyll. *Photochem. Photobiol.* 14, 95-112.

Rio, Y., Rodriguez-Morade, M. S. and Torres, T. 2008. Modulating the Electronic Properties of Porphyrinoids: A Voyage from the Violet to the Infrared Regions of the Electromagnetic Spectrum. *Org. Biomol. Chem.* 1877-1894.

Wamser, C. C, Kim, H.-S. and Lee, J.-K. 2002. Solar Cells with Prophyrin Sensitization. *Opt. Mat.* 21, 221-224.

Wang, Z., Medforth, C. J. and Shelnutt, J. A. 2004. Porphyrin Nanotubes by Ionic Self-Assembly. *J. Am. Chem. Soc.* 126, 15954-15956.